

Thermal Insulation Choice for Solid Rockets: A Study on Liner Material Properties and Design Impact

Omar Lamini^{1*}, Khaled Teffah¹, Hemza Layachi¹

¹Algerian Space Agency, Bouzareah Algiers, Algeria

ARTICLE INFO

Article history:

Received 22 July 2025
Revised 5 October 2025
Accepted 24 January 2026
Online first
Published 15 May 2026

Keywords:

Casing liner
Solid motor insulation
Rocket design
Rocket flight performance
Model rocket

DOI:

10.24191/jmeche.v23i2.9110

ABSTRACT

The materials used in the construction of solid rockets are critical to their overall and final performance. Among the most important components is the liner of the casing, which shields the casing from the heat generated during the solid propellant combustion. Various types of liners are available, and selecting one with high thermal performance is essential to optimizing the design and flight performance of the rocket. In this study, the effect of different liners with different materials on the overall weight and the final design of the rocket, which are key factors in its flight capabilities, is numerically investigated. Using OpenRocket, a preliminary rocket design is first performed by selecting a solid motor and constructing the remaining components. Next, thermal simulations are conducted in ANSYS Steady-State Thermal to evaluate three liner options with low, medium, and high thermophysical properties. The results show that each liner requires a specific thickness to keep the casing within safe temperature limits. Finally, these thicknesses are re-evaluated in OpenRocket to assess their impact on rocket flight performance. These findings demonstrate that the liner selection has significant effects on key flight parameters such as apogee, maximum velocity, and time to apogee. Furthermore, a poor liner choice could risk the entire success of the flight mission.

INTRODUCTION

The design and performance of solid rocket motors are critical components in the success of aerospace missions, whether they involve launching satellites, propelling space exploration vehicles, or delivering payloads with precision (Kubota, 2004; Zeping et al., 2017). Central to the functionality of these motors is the casing, which not only houses the solid propellant but also provides structural integrity under the extreme conditions encountered during ignition, combustion, and thrust (Dinesh Kumar et al., 2016; Mahadevan et al., 2022; Muhammad et al., 2022). One of the most challenging aspects of solid rocket motor design is managing the intense thermal loads generated by the combustion process (Ahmed & Hoa, 2012; Mohamed et al., 2021). The selection of an appropriate liner for the casing is, therefore, a crucial factor in

^{1*} Corresponding author. *E-mail address:* olamini@asal.dz
<https://doi.org/10.24191/jmeche.v23i2.9110>

ensuring the operational reliability of the rocket and its overall performance (Ahmad et al., 2021; Ahmed & Hoa, 2012; George et al., 2018; Natali et al., 2013).

Solid rocket motor casings are typically constructed from high-performance materials such as nickel-based superalloys, high-strength steels, and advanced composites, chosen for their ability to withstand high temperatures and mechanical stresses (Amado, 2016; Lauder, 1995; Rajan & Narasimhan, 2002). However, the effectiveness of these materials is significantly determined by the type of the liner applied to them (Elashker et al., 2023; Rheeder, 2022). The liner must mitigate the extreme heat generated during the burning phase, preventing thermal degradation of the casing material, preserving structural integrity, and minimizing heat transfer to the exterior, which could adversely affect the payload or the surrounding components (Alaghemandi & Alamandi, 2025; Amado et al., 2020; Spirnak, 2018). The thermophysical properties of the liner, such as thermal conductivity and density play a crucial role in determining how efficiently the liner could protect the casing during combustion (Lamini et al., 2021).

The choice of the liner is a delicate balance between thermal performance, weight, and manufacturability (Shvydyuk et al., 2023; Uyanna & Najafi, 2020). Heavier or bulkier thermal protection might offer superior heat resistance but could compromise the thrust-to-weight ratio and maneuverability of the rocket. Conversely, lighter materials may provide better performance characteristics but may not offer sufficient thermal protection, risking the integrity of the casing (Blosser, 1997; Cheng et al., 2021; Dorsey et al., 2004; Shukla et al., 2014). These trade-offs become even more critical when considering the broader challenges facing the aerospace industry in recent years leading to perform an undesirable rocket design.

Recent global events, particularly the COVID-19 pandemic and the ongoing Russia-Ukraine conflict, in addition to the economic conflict between China and the United States, have exacerbated supply chain disruptions across various industries, including aerospace (Roscoe et al., 2022; Wilson, 2010). The aerospace industry, heavily reliant on complex, international supply chains, has faced significant challenges in sourcing critical materials and components, including those used in thermal protection systems. These disruptions have been particularly impactful in developing countries, where access to advanced materials and technologies is often limited even in the best of times (Oyewole, 2023). The resulting scarcity of high-performance liner materials not only threatens to delay aerospace projects in such countries but also raises the risk of compromises in material selection, potentially impacting the safety and effectiveness of rocket designs.

In this context, the need for a comprehensive understanding of different liners becomes even more urgent (Ahmad et al., 2021; Elashker et al., 2023). This study focuses on the numerical analysis of three distinct liner options applied to a single casing material. By isolating the thermal protection variable while keeping the casing material constant, the research aims to provide insights into how different liner choices could affect the overall design of the rocket and key performance metrics such as casing temperature, launch velocity, apogee, and the overall performance of the rocket. These simulations are designed to replicate the severe thermal environments encountered by solid rocket motors, providing valuable data to guide material and design choices.

The findings of this research will contribute to the development of more resilient and efficient solid rocket motors, particularly in the context of supply chain uncertainties. By identifying optimal liners strategies that maximize performance while considering material availability, this study seeks to enhance the performance and safety of rockets, with potential applications extending from space exploration to commercial satellite and payload deployment at different altitudes, in both developed and developing countries. The results could lead to significant improvements in thermal management strategies, reducing weight, enhancing structural integrity, and ultimately improving mission success rates, even amidst global supply challenges.

ROCKET DESIGN AND THERMAL ANALYSIS METHODOLOGY

The open-source software OpenRocket was used to design the solid rocket model for this study (Niskanen, 2009). A simplified design was employed, incorporating the essential components of a solid rocket: motor, casing, liner, nose cone, parachute, payload, and fins. Fig. 1 presents a preliminary design of the rocket, illustrating the overall layout and configuration of its key elements. The design process began with the selection of the solid motor, which serves as the core of the rocket. The selected solid motor has an outer diameter of 98 mm and a length of 1010 mm. All other components were constructed based on this motor to ensure optimal integration and performance.

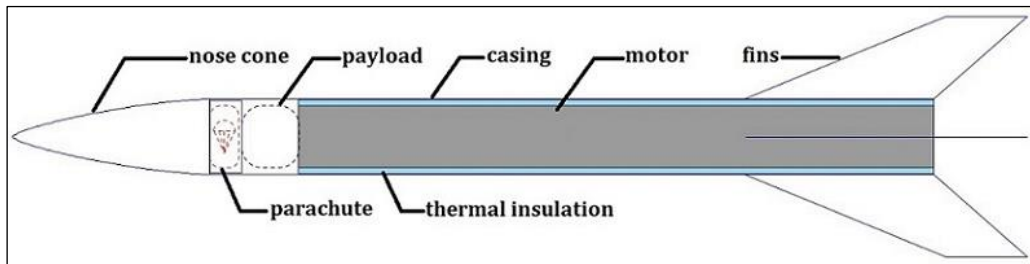


Fig. 1. Preliminary design of the solid rocket.

Since the primary objective of this study is to evaluate the effect of the motor liner on rocket performance, the thermal simulation focuses exclusively on the interaction between the insulation and the casing with the applied working conditions. Fig. 2(a) illustrates the assembly of the liner and the casing, where the casing (light gray) is modeled with a thickness of 1 mm, and the thermal insulation, or liner (dark gray), is represented with an initial arbitrary thickness.

The thickness of the liner plays a crucial role in protecting the casing from excessive heat. A perfect thermal contact was assumed at the liner–casing interface, this assumption is common in preliminary design studies. Although thermal contact resistance may vary depending on liner composition and manufacturing processes, applying the same interface condition across all materials ensures consistent comparison of their thermal performance. In order to find an adequate liner thickness in our study, the simulation starts with a thickness of 1 mm. If results show that the casing temperature exceeds its allowable limit, the liner thickness is incrementally increased, and the simulation is repeated. This iterative process continues until the casing remains within its thermal safety range.

The thermal boundary conditions were set to replicate critical real-world conditions for a static firing test of a solid rocket motor. Ambient conditions were applied to the outer surface, with an external air temperature of 25 °C. The heat transfer coefficient in such conditions typically ranges between 0 and 25 W/m² °C (Roncati, 2013). To simplify the simulation, a representative value of 20 W/m² °C was selected. The inner surface of the liner was subjected to a temperature of 2000 °C to simulate the extreme heat during combustion. Although the firing temperature can reach up to 3000 °C depending on the motor's intended application, design, and propellant formulation (Fernandes et al., 2022), a conservative yet representative value was chosen for this study. The applied working conditions are shown in Fig. 2(b).

Using the physical characteristics of the model and considering the uniform temperature distribution on the inner liner surface and uniform ambient conditions on the outer casing surface, the temperature distribution across the two layers, namely the liner and the casing, can be modeled as a linear function in cylindrical coordinates (Vicentin et al., 2019). This approach follows Fourier's law of heat conduction (Bergman et al., 2011), and the corresponding heat flux through both the liner and the casing is expressed as:

$$q = -\lambda \frac{dT}{dr} \quad (1)$$

where q is the heat flux, λ is the thermal conductivity of the liner or the casing, T is the temperature, and r is the radial coordinate. The temperature profile through the liner and casing is given by:

$$T(r) = T_{in} - \frac{q}{\lambda_l} r \quad \text{for } 49 \text{ mm} \leq r \leq e_l \quad (2)$$

$$T(r) = T_l - \frac{q}{\lambda_c} (r - e_l) \quad \text{for } e_l \leq r \leq e_l + e_c \quad (3)$$

where T_{in} is the temperature at the inner liner surface (2000 °C), λ_l is the liner's thermal conductivity, 49 mm is the outer radius of the selected solid motor and the inner radius of the liner (Fig. 2(b)), e_l is the liner thickness, T_l is the temperature at the liner-casing interface ($r = e_l$), and e_c is the casing thickness (1 mm). At the outer surface, Newton's law of convection applies:

$$q = h_{amb}(T_c - T_{amb}) \quad (4)$$

where h_{amb} is the ambient heat transfer coefficient (20 W/m² °C), T_c is the casing's outer temperature, and T_{amb} is the ambient air temperature (25 °C). Combining Equations (1 to (4), the total heat flux is given by:

$$q = \frac{T_{in} - T_{amb}}{\frac{e_l}{\lambda_l} + \frac{e_c}{\lambda_c} + \frac{1}{h}} \quad (5)$$

The temperature gradient through the liner and casing is then:

$$\frac{dT}{dr} = \begin{cases} -\frac{q}{\lambda_l} & \text{if } 49 \text{ mm} \leq r \leq e_l \\ -\frac{q}{\lambda_c} & \text{if } e_l \leq r \leq e_l + e_c \end{cases} \quad (6)$$

This mathematical model, described by Equations 1 to 6, was used to analyze the system under steady-state conditions. The steady-state assumption is appropriate because the objective of the present study is to assess the casing temperature under critical peak-heating conditions, which occur near the maximum chamber temperature during combustion. Although the combustion process is transient, the peak combustion temperature remains approximately constant for a short but enough time during the combustion, and this period governs the maximum thermal load transmitted through the insulation. Steady-state modelling is therefore suitable for estimating the maximum casing temperature under these peak conditions and is commonly used in preliminary design assessments where the focus is on sizing insulation materials rather than resolving the full transient evolution. In order to optimize computational efficiency, the analysis focused on a reduced section of the rocket, specifically a 101 mm length and 38° arc of both the casing and liner components, representing 10% of their full dimensions as shown in Fig. 2(b). Once the rocket design was finalized and the operating conditions were defined, thermal simulations were performed using the commercial CFD package ANSYS Steady-State Thermal.

The casing material selected for this study was Inconel 718, a nickel-based superalloy widely used in high-temperature aerospace applications. Its thermophysical properties are detailed in Table 1, with a

maximum working temperature of 700 °C, which serves as the thermal limit during combustion. Three liner materials, each with distinct thermophysical properties (low, medium, and high conductivity), were selected for the thermal simulations. These materials, commonly used in solid rocket engineering, are detailed in Table 1. The objective of the simulations was to determine the appropriate liner thickness that ensures sufficient thermal protection while minimizing added weight and bulk.

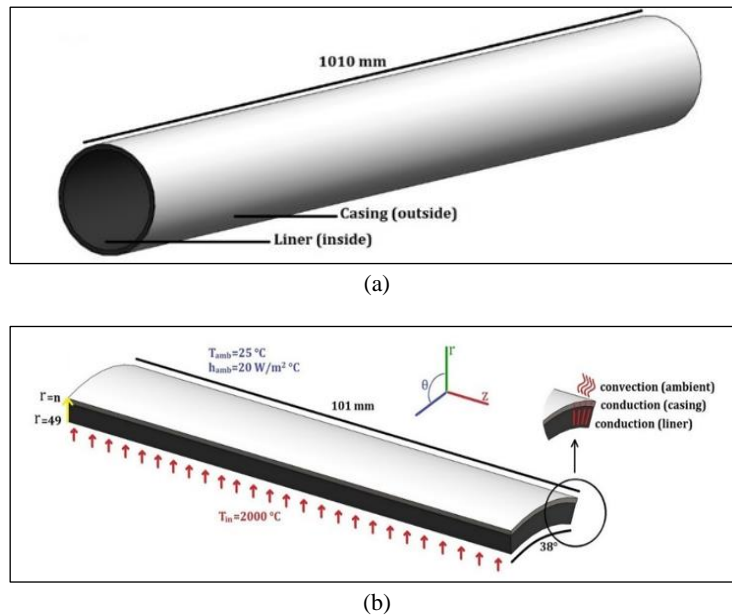


Fig. 2. Preliminary design of the liner and the casing: (a) full size of the casing and the liner and (b) the part to be numerically tested of the casing and the liner with the applied working conditions.

Table 1. Thermophysical properties of the casing and the liners (Chung, 1994; Special Metal Corporation, 2007; US Department of Defense, 1998; Grimvall, 1999; Rice, 2017)

Material	Density (g/cm ³)	Thermal conductivity (W/m·K)	Specific heat capacity (J/Kg·K)
Inconel 718	8.19	13	435
Ceramic fibers	0.2	0.04	1000
Carbon fibers	1.6	0.1	800
Refractory ceramics	5	0.3	700

A mesh sensitivity analysis was conducted to check the accuracy of the thermal simulation. Four mesh densities: 5, 10, 20, and 40 layers per millimetre were evaluated in the radial direction as heat transfer occurs predominantly from the inner liner surface toward the outer casing surface. Coarser meshes (5 and 10 layers/mm) produced visibly non smooth temperature gradients within the thin Inconel casing and insufficient resolution of the steep temperature drop across the liner – casing interface. In contrast, the difference between the 20 and 40 layers per millimetre meshes was negligible with a maximum casing temperature difference of less than 0.5 °C. Therefore, a density of 20 layers per millimetre was selected as the optimal compromise between accuracy and computational efficiency. The tested mesh configurations are shown in Fig. 3, and the corresponding temperature distributions are presented in Fig. 4. .

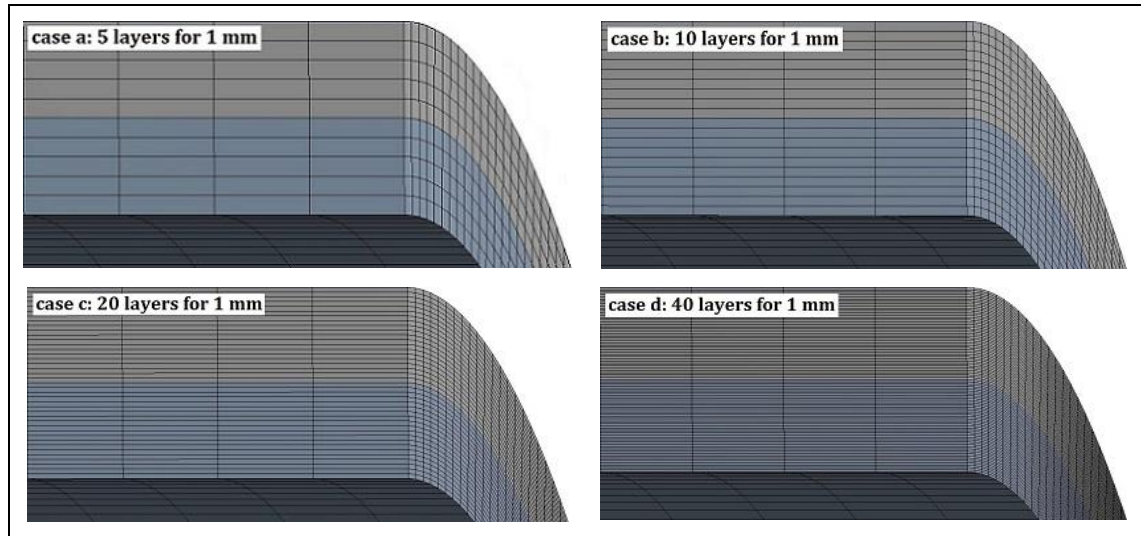


Fig. 3. The four mesh densities were used to test the mesh-sensitivity.

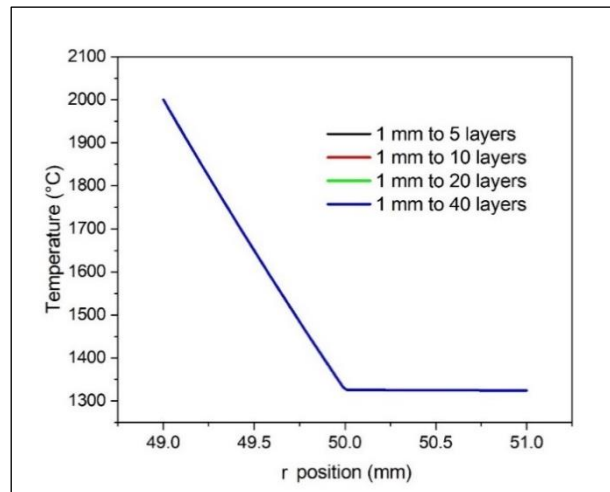


Fig. 4. The four mesh densities resulted in the same temperature distribution.

RESULTS AND DISCUSSION

Effect of the liner thermal properties on casing temperature

Fig. 5 illustrates the effect of liner materials with varying thermal properties on the temperature gradient across a 1 mm thick liner and casing. Although this thickness is insufficient for thermal protection (as the maximum working temperature of Inconel 718 is 700 °C), the comparison highlights the influence of liner thermophysical properties on the casing temperature distribution.

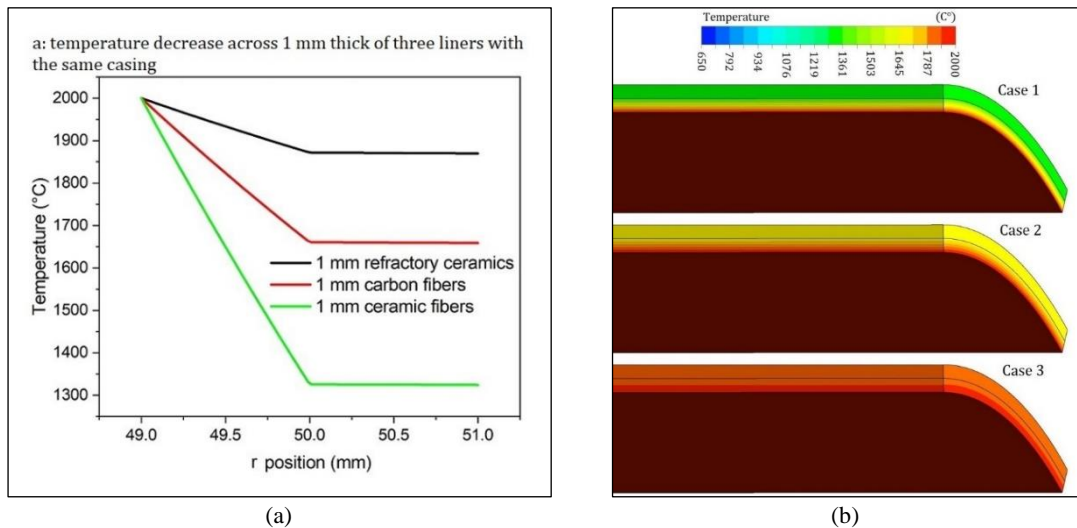


Fig. 5. (a) Temperature decreases across the liner and the casing (both are 1 mm thick) and (b) temperature contours of 1 mm thick Inconel 718 casing with 1 mm thick of (case 1) ceramic fibers, (case 2) carbon fibers and finally (case 3) refractory ceramics' liners having different thermal properties.

The liner materials analyzed include ceramic fibers (low thermal conductivity, $\lambda = 0.04$ W/m·K), carbon fibers (medium thermal conductivity, $\lambda = 0.1$ W/m·K), and refractory ceramics (high thermal conductivity, $\lambda = 0.3$ W/m·K), while the casing is made of Inconel 718 ($\lambda = 13$ W/m·K). The results reveal that ceramic fibers achieve the largest temperature drop, decreasing from 2000 °C at the inner surface to 1326 °C at the outer surface, a reduction of 674 °C. Across the Inconel casing, the temperature decreases by only 2 °C to 1324 °C. Carbon fibers show a moderate drop, from 2000 °C to 1661 °C (436 °C reduction), and 2 °C across the casing. Refractory ceramics exhibit the smallest drop, from 2000 °C to 1872 °C (128 °C), with 2 °C across the casing.

These findings underscore the importance of liner thermal properties in casing protection. Liners with lower conductivity provide effective protection with thinner layers, whereas liners with higher conductivity require greater thickness, affecting rocket performance and efficiency, as will be discussed in the next sections.

Thermal protection of the casing with the three liners

Given the distinct thermal properties of the liners used in this study, varying thicknesses (denoted as L_t in the Fig. 6) are necessary to provide adequate protection for the casing against thermal failure. The initial thickness tested in the simulations is always 1 mm. After evaluating the results, a new thickness is determined and tested iteratively until the casing is effectively thermally protected.

Fig. 6(a) presents the temperature evolution along the ceramic fibers' liner and the casing, which is consistently made of Inconel 718. For the first liner thickness L_t of 1 mm (indicated in red), the temperature decreases from 2000 °C at the inner surface of the liner to 1326 °C at the outer surface. While this represents a significant reduction, it remains insufficient for the thermal protection of the casing, necessitating a thicker liner. The subsequent thickness tested is 3 mm, as indicated by the green curve, which shows a temperature drop from 2000 °C to 791 °C; this value still exceeds the safe operating temperature for Inconel 718 (700 °C). Next, a thickness of 3.5 mm is evaluated, yielding a temperature of 714 °C. Although this temperature approaches the required thermal protection limit, it still exceeds 700 °C. Upon testing a 4 mm

liner thickness, the temperature reduces to 657 °C, confirming that the casing is adequately thermally protected with this thickness of ceramic fibers.

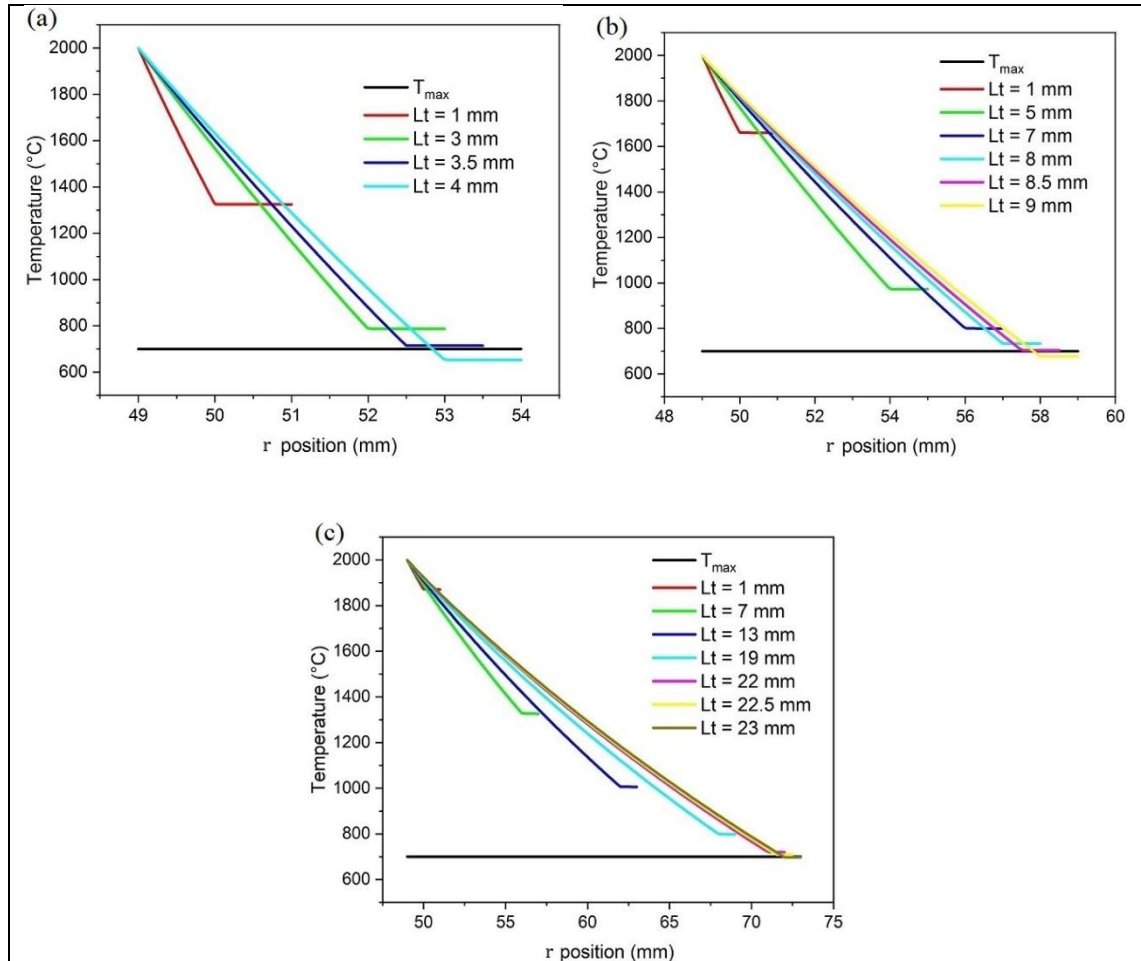


Fig. 6. Temperature decreases across different liners. Maximum allowed temperature of the casing is 700 °C (in black). For different liners, different thicknesses are required to achieve thermal protection: (a) ceramic fibers, (b) carbon fibers, and (c) refractory ceramics.

Fig. 6(b) illustrates the temperature evolution across the carbon fibers liner at various thicknesses, including 1 mm, 5 mm, 7 mm, 8 mm, 8.5 mm, and finally 9 mm. The resulting temperatures decrease from 2000 °C at the inner surface to 1661 °C, 976 °C, 802 °C, 734 °C, 708 °C, and ultimately 680 °C, respectively. It is evident that to ensure adequate thermal protection of the casing with a carbon fibers liner, a thickness of 9 mm is required due to its moderate thermal conductivity.

Fig. 6(c) displays the temperature reduction across the refractory ceramics' liner with increasing thicknesses of 1 mm, 7 mm, 13 mm, 19 mm, 22 mm, 22.5 mm, and finally 23 mm. The corresponding temperatures are 1872 °C, 1329 °C, 1007 °C, 800 °C, 720 °C, 712 °C, and ultimately 698 °C, respectively. The refractory ceramics exhibit poor thermal protection properties (high conductivity), necessitating a significantly thicker layer to maintain the casing temperature below 700 °C.

Figs. 6(a-c) illustrate temperature gradients for different liners, highlighting the considerable differences in liner thickness required for adequate thermal protection of the casing. Notably, when ceramic fibers are employed as a liner, a thickness of only 4 mm suffices. In contrast, a thickness of 9 mm is necessary when utilizing carbon fibers, while refractory ceramics require an extensive thickness of 23 mm. These differences in liner thickness will substantially influence the final weight of the rocket and its overall performance, as will be discussed in the next section.

Influence of the liner choice on the overall performance of the rocket

Fig. 7 illustrates a comparison of different solid rockets utilizing various types of liners, each with distinct thermal properties. Considering a casing thickness of 1 mm, it is evident from Fig. 7 that the choice of liner significantly impacts the outer diameter of the casing. When ceramic fibers, known for their low thermal conductivity ($\lambda = 0.04 \text{ W/m}\cdot\text{K}$), are employed as the liner, the outer diameter of the casing measures only 108 mm. In contrast, using carbon fibers with a medium thermal conductivity ($\lambda = 0.1 \text{ W/m}\cdot\text{K}$) results in an outer diameter of 119 mm. Conversely, when refractory ceramics, characterized by high thermal conductivity ($\lambda = 0.3 \text{ W/m}\cdot\text{K}$), are used, the outer diameter of the casing expands to 146 mm. This increase in diameter consequently elevates the volume and weight of the casing, significantly affecting the overall performance of the solid rocket.

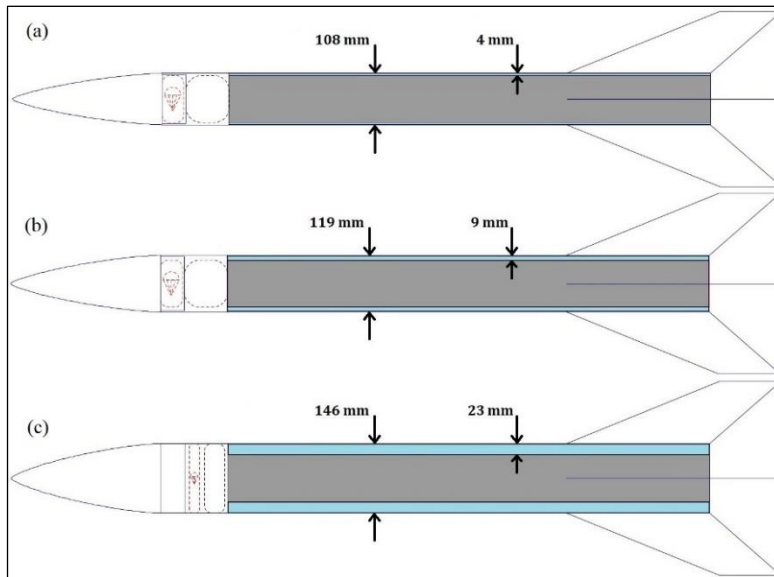


Fig. 7. Final design of solid rockets with different liners: (a) solid rocket with ceramic fibers as a liner, (b) solid rocket with carbon fibers as a liner and (c) solid rocket with refractory ceramics as a liner.

The performance data presented in Table 2 and Fig. 8 were obtained from OpenRocket trajectory simulations using the rocket geometries and total masses calculated in the previous section. Table 2 presents various performance parameters that highlight the relationship between the weight and the overall performance of the solid rocket. The total mass of the rocket utilizing ceramic fibers as a liner is 22798 g. When carbon fibers are employed, the total mass rises to 28272 g, representing a 24% increase compared to the rocket with ceramic fibers. Furthermore, the total mass with refractory ceramics as a liner escalates to 67730 g, reflecting an approximate 197% increase relative to the rocket with ceramic fibers and about 140% more than the rocket with carbon fibers.

Table 2. Rocket performance parameters influenced by different liners

Parameter	Ceramic fibers	Carbon fibers	Refractory ceramics
Total mass of the rocket (g)	22798	28272	67730
Launch velocity (m/s)	31.5	27.7	17.4
Apogee (m)	1602	1599	880
Time to apogee (s)	13.5	14.3	12.9
Maximum velocity (m/s)	490	386	148
Maximum acceleration (m/s ²)	562	440	167
Flight time (s)	37.7	37.1	27.2
Ground hit velocity (m/s)	85.2	96.7	113

It is observed that the launch velocity, maximum velocity, and ground impact velocity are all dependent on the weight of the solid rocket. The launch velocity is recorded at 31.5 m/s for the rocket with ceramic fibers as a liner, decreasing to 27.7 m/s with carbon fibers, and further dropping to 17.4 m/s with refractory ceramics. Additionally, the maximum velocity of the rocket with ceramic fibers is 490 m/s, which reduces to 386 m/s when carbon fibers are used and declines to 148 m/s with refractory ceramics. The ground impact velocity, however, exhibits an opposite trend: the rocket with ceramic fibers has an impact velocity of 85.2 m/s, increasing to 96.7 m/s with carbon fibers and rising to 113 m/s with refractory ceramics. This variation is attributed to the weight of the rocket influencing its descent towards the ground. The maximum acceleration of the rocket with ceramic fibers is 562 m/s², decreasing to 440 m/s² with carbon fibers and further diminishing to 167 m/s² with refractory ceramics.

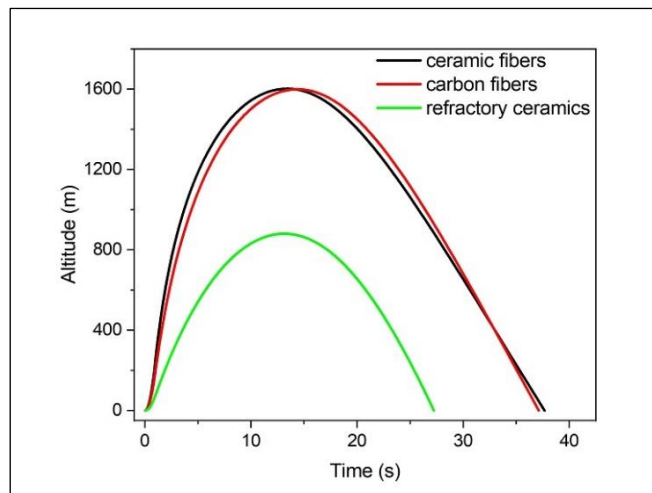


Fig. 8. Final design of solid rockets with different liners.

Fig. 8. depicts the effect of the weight of the rocket on its flight performance. The three curves reveal that the rocket exhibits only a small difference in apogee when utilizing ceramic fibers versus carbon fibers as liners, reaching 1602 m in 13.5 s with ceramic fibers and 1599 m in 14.3 s with carbon fibers. However, a notable disparity arises when refractory ceramics are used as a liner, resulting in a maximum apogee of only 880 m in 12.9 s. Moreover, the total flight time is longest for the rocket with ceramic fibers as a liner, at 37.7 s until it impacts the ground. The difference is minimal when using carbon fibers as a liner, with a total flight time of 37.1 s, attributable to the heavier rocket descending more rapidly. Conversely, the rocket

with refractory ceramics, due to its lower apogee and increased weight, exhibits the shortest flight time of 27.2 s.

Rocket performance optimization with payload adjustments

In the previous section, the payload weight for all three rockets was fixed at 5000 g, resulting in variations in apogee due to differences in the overall rocket weight. Heavier rockets reached lower altitudes, primarily because of the differences in liner thickness and density, which affected the casing size and, consequently, the final weight of the rocket. In this section, the objective is to achieve a target apogee of 1000 m by adjusting the payload weight for each of the three rockets, which are equipped with different liners. While no maximum payload weight is imposed, looking for a maximum, the minimum payload weight is set at 1000 g. For each case, the casings are thermally protected according to the thicknesses recommended previously: 4 mm for ceramic fibers, 9 mm for carbon fibers, and 23 mm for refractory ceramics. Thus, the only variable being adjusted is the payload weight, while the rocket bodies remain as shown in Fig. 7.

Table 3 presents the results for achieving the target apogee of 1000 m. The rocket with ceramic fibers as the liner is capable of carrying a payload of up to 43600 g to an altitude of 1000 m. The rocket with carbon fibers can carry a payload of 38000 g to the same apogee. However, even with the minimum payload weight of 1000 g, the rocket equipped with refractory ceramics fails to reach the target altitude, achieving only 953 m. This shows that the rocket with refractory ceramics, despite reducing the payload to the lowest possible limit, is unable to meet the 1000 m requirement.

Table 3. Key performance of the rockets with a 1000 m apogee target

Parameter	Ceramic fibers	Carbon fibers	Refractory ceramics
Payload weight (g)	43600	38000	1000
Apogee (m)	1000	1000	953
Time to apogee (s)	13.8	13.8	13.6
Launch velocity (m/s)	18.7	18.8	18.2
Maximum velocity (m/s)	165	166	159
Maximum acceleration (m/s ²)	186	187	179
Flight time (s)	29	29	28.3
Ground hit velocity (m/s)	116	116	115

Additionally, Table 3 highlights that the performance of the rockets using ceramic fibers and carbon fibers as liners is quite similar. In contrast, the rocket with refractory ceramics as liner shows significantly lower performance, even with a minimal payload. Fig. 9 further illustrates this point, as the altitude versus time curves for rockets with ceramic and carbon fibers nearly overlap, while the rocket with refractory ceramics exhibits a noticeably lower trajectory.

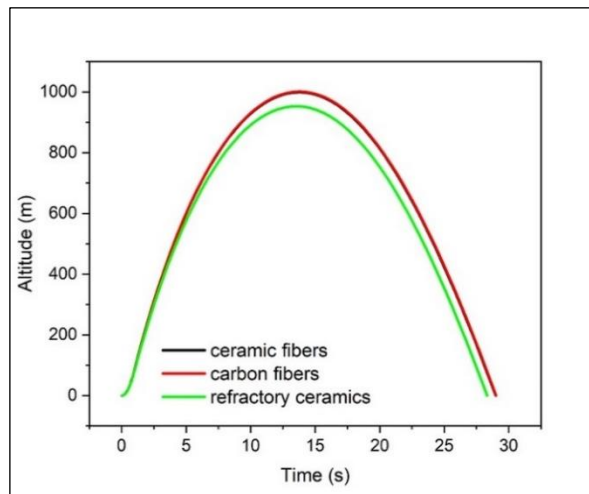


Fig. 9. Altitude and flight time of rockets carrying payloads with different weights.

CONCLUSION AND FUTURE PROSPECTS

This study investigated the influence of liner materials on the thermal protection and performance of solid rocket casings. Ceramic fibers, with their low thermal conductivity, provided the most efficient thermal protection, requiring the thinnest layer to shield the Inconel 718 casing effectively. Conversely, refractory ceramics, with higher thermal conductivity, demanded significantly thicker layers, which increased the overall weight of the rocket and compromised its performance.

The impact of liner thickness and material properties was evident in key performance parameters, such as launch velocity, maximum velocity, apogee, and total flight time. Rockets using ceramic fiber liners achieved superior performance, including higher apogees and higher launch velocity. Similarly, rockets with carbon fiber liners demonstrated acceptable performance but required greater liner thicknesses. In contrast, rockets with refractory ceramic liners failed to meet the target apogee of 1000 m, even with the lightest payload, underscoring the trade-offs between thermal protection and rocket total weight.

While experimental validation was not included in the present work, all liner materials were evaluated under identical thermal loads, boundary conditions, and modelling assumptions. This controlled comparative framework ensures that the relative differences and engineering trends reported here remain meaningful for preliminary design decisions. Future work will incorporate firing-test data to further improve the fidelity of the numerical predictions.

Based on the results obtained, ceramic fibers represent the most effective liner material for achieving both adequate thermal protection and favorable flight performance. However, the technically optimal solution may not always constitute the optimal engineering choice. Practical factors such as manufacturing complexity, material availability, fabrication infrastructure, and overall cost can shift the selection toward materials with lower manufacturing complexity or more reliable supply chains.

Beyond thermal protection, overall rocket performance depends on the integration and optimization of multiple subsystems. Inefficient electronic shielding can compromise guidance and control, while suboptimal solid propellant formulation may impact thrust and burn rate, increasing the risk of mission failure. To refine thermal protection strategies further, future research will incorporate transient thermal simulations to capture the heating conditions experienced during dynamic firing tests. Additionally,

temperature-dependent material properties will be integrated into the analysis to enhance the accuracy of thermal predictions. These advancements, combined with the exploration of novel materials (Tahir & Zubir, 2025), will contribute to the development of more efficient and reliable solid rocket systems ensuring optimal performance.

ACKNOWLEDGMENT

The author expresses gratitude to the Satellite Development Center – Oran for their support in providing the necessary means (ANSYS Steady-State Thermal) to conduct the numerical simulations.

CONFLICT OF INTEREST STATEMENT

The author(s) declared no potential conflicts of interest with respect to the research, authorship, and/or publication of this article.

AUTHORS' CONTRIBUTION

The authors confirm their contribution to the paper as follows: study conception, design, analysis, interpretation and paper writing: Omar Lamini; analysis, revision, improving writing quality: Khaled Teffah; analysis, revision, improving writing quality: Hemza Layachi. All authors reviewed the results and approved the final version of the manuscript.

DECLARATION OF GENERATIVE AI IN THE WRITING PROCESS

During the preparation of this work, the authors used an AI tool in order to enhance the readability and language quality of the work. After using this tool, the authors reviewed and edited the content as needed and take full responsibility for the content of the publication.

DATA AVAILABILITY/ SUPPLEMENTARY MATERIALS

All data generated or analysed during this study are included in this published article [and its supplementary information files].

ETHICS STATEMENT

This study is based on computational simulations and does not involve human participants, animal subjects, clinical data, or any personally identifiable information. As such, no ethical approval from an institutional review board or ethics committee was required. All simulations were conducted in accordance with standard scientific computing practices.

REFERENCES

- Ahmad, S., Ali, S., Salman, M., & Baluch, A. H. (2021). A comparative study on the effect of carbon-based and ceramic additives on the properties of fiber reinforced polymer matrix composites for high temperature applications. *Ceramics International*, 47(24), 33956-33971.
- Ahmed, A. F., & Hoa, S. V. (2012). Thermal insulation by heat resistant polymers for solid rocket motor insulation. *Journal of Composite Materials*, 46(13), 1549-1559.
- Alaghemandi, M., & Alamandi, M. (2025). Heat transfer in composite materials: mechanisms and applications [Preprint]. arXiv. <https://doi.org/10.48550/arXiv.2501.15231>
- Amado, J. C. Q., Ross, P. G., Sanches, N. B., Pinto, J. R. A., & Dutra, J. C. N. (2020). Evaluation of elastomeric heat shielding materials as insulators for solid propellant rocket motors: a short review. *Open Chemistry*, 18(1), 1452-1467.
- Amado, J. C. Q. (2016). Manufacture and testing of lightweight tubes for rocketry and centrifuges. *Lightweight composite structures in transport* (pp. 421-437). Elsevier.
- Bergman, T. L., Lavine, A. S., Incropera, F. P., & Dewitt. (2011). *Fundamentals of heat and mass transfer*. (7th Ed.). John Wiley & Sons.
- Blosser, M. L. (1997). Development of metallic thermal protection systems for the reusable launch vehicle. *AIP Conference Proceedings*, 387(1), 1125-1144.
- Cheng, H., Fan, Z., Hong, C., & Zhang, X. (2021). Lightweight multiscale hybrid carbon-quartz fiber fabric reinforced phenolic-silica aerogel nanocomposite for high temperature thermal protection. *Composites Part A: Applied Science and Manufacturing*, 143, 106313.
- Chung, D. D. L. (1994). *Carbon fiber composites*. Butterworth-Heinemann.
- Dinesh Kumar, B., Shishira Nayana, B., & Shravya Shree, D. (2016). Design and structural analysis of solid rocket motor casing hardware used in aerospace applications. *Journal of Aeronautics & Aerospace Engineering*, 5(2), 166.
- Dorsey, J. T., Poteet, C. C., Wurster, K. E., & Chen, R. R. (2004). Metallic thermal protection system requirements, environments, and integrated concepts. *Journal of Spacecraft and Rockets*, 41(2), 162-172.
- Elashker, A., Zaghoul, B., Eldakhkhny, A., Gobara, M., & Mokhtar, M. (2023). Study of thermal protection materials in solid propellant rocket engines. *International Conference on Aerospace Sciences and Aviation Technology* (pp. 1-10). IOP Publishing.
- Fernandes, F. A. C., Souto, C. A., & Pirk, R. (2022). Static firing tests of solid propellant rocket motors: uncertainty levels of thrust measurements. *Journal of Aerospace Technology and Management*, 14, e2022.
- George, K., Panda, B. P., Mohanty, S., & Nayak, S. K. (2018). Recent developments in elastomeric heat shielding materials for solid rocket motor casing application for future perspective. *Polymers for Advanced Technologies*, 29(1), 8-21.
- Grimvall, G. (1999). *Thermophysical properties of materials*. Elsevier.
- Kubota, N. (2004). Principles of solid rocket motor design. *Journal of Pyrotechnics*, 20, 27-50.

- Lamini, O., Wu, R., & Zhao, C. (2021). Experimental study on the effect of the liquid/ surface thermal properties on droplet impact. *Thermal Science*, 25(1B), 705-716.
- Lauder, A. J. (1995). Manufacture of rocket motor cases using advanced filament winding processes. *Materials and Manufacturing Process*, 10(1), 75-87.
- Mahadevan, P., Ravishankar, A., & Gunasekaran, M. (2022). Design and analysis of solid rocket motor casing. *Indian Conference on Applied Mechanics* (pp. 267-272). Springer.
- Mohamed, W. M. W., Salleh, Z., Hamid, A. H. A., Muhammad, M. A., & Salleh, N. A. (2021). Thermal analysis on solid rocket motor casing. *International Transaction Journal of Engineering, Management, & Applied Sciences & Technologies*, 12(9), 1-13.
- Muhammad, M. A., Salleh, Z., Hamid, A. H. A., Sujana, M. J., & Kamaludin, K. (2022). Finite element analysis for rocket motor case under internal pressure and thermal loads. *Journal of Applied Engineering Design and Simulation*, 2(2), 11-21.
- Natali, M., Rallini, M., Puglia, D., Kenny, J., & Torre, L. (2013). EPDM based heat shielding materials for solid rocket motors: a comparative study of different fibrous reinforcements. *Polymer Degradation and Stability*, 98(11), 2131-2139.
- Niskanen, S. (2009). Development of an Open Source model rocket simulation software [Master's thesis, Helsinki University of Technology]. Retrieved from <https://openrocket.sourceforge.net/thesis.pdf>
- Oyewole, S. (2023). The African orbital journey in space age: from spectator to participant. *Vanguardia Dossier*, 88(15), 72-75.
- Rajan, K. M., & Narasimhan, K. (2002). An approach to selection of material and manufacturing processes for rocket motor cases using weighted performance index. *Journal of Materials Engineering and Performance*, 11(4), 444-449.
- Rheeder, A. (2022). Development and evaluation of thermal protection material for solid rocket motors [Master's thesis, Stellenbosch University]. Retrieved from <http://hdl.handle.net/10019.1/124739>
- Rice, R. W. (2017). Porosity of ceramics. Properties and applications. CRC Press.
- Roncati, D. (2013). Iterative calculation of the heat transfer coefficient. *Progettazione Ottica Roncati*.
- Roscoe, S., Aktas, E., Petersen, K. J., Skipworth, H. D., Handfield, R. B., & Habib, F. (2022). Redesigning global supply chains during compounding geopolitical disruptions: the role of supply chain logics. *International Journal of Operations & Production Management*, 42(9), 1407-1434.
- Shukla, A. K., Sharma, V. M. J., Murty, S. V. S. N., Narayanan, P. R., & Sharma, S. C. (2014). Integrity of structural and thermo-structural materials for Indian space programme. *Procedia Engineering*, 86, 8-17.
- Shvydyuk, K. O., Nunes-Pereira, J., Rodrigues, F. F., & Silva, A. P. (2023). Review of ceramic composites in aeronautics and aerospace: a multifunctional approach for TPS, TBC and DBD applications. *Ceramics*, 6(1), 195-230.
- Special Metals Corporation. (2007). Inconel® alloy 718 (Technical bulletin). Special Metals.
- Spirnak, J. R. (2018). Development, modeling and testing of thermal protection systems in small, slow-burning solid rocket motors [Bachelor's thesis, Massachusetts Institute of Technology]. Retrieved from <http://hdl.handle.net/1721.1/118689>

- Tahir, N. A., & Zubir, S. A. (2025). Development of high-performance HTPB and cerium oxide-based polyurethane composite liners for solid rocket motors. *Polymers for Advanced Technologies*, 36(2), e70117.
- US Department of Defense. (1998). *Military handbook: Metallic materials and elements for aerospace vehicle structures* (Vol. 1).
- Uyanna, O., & Najafi, H. (2020). Thermal protection systems for space vehicles: a review on technology development, current challenges and future prospects. *Acta Astronautica*, 176, 341-356.
- Vicentin, I. C. F. S., Marchi, C. H., Foltran, A. C., Moro, D., Silva, N. D. P., Campos, M. C., Araki, L. K., & Diógenes, A. N. (2019). Theoretical and experimental heat transfer in solid propellant rocket engine. *Journal of Aerospace Technology and Management*, 11, e3819.
- Wilson, B. K. (2010). Risk from network disruptions in an aerospace supply chain [Master's thesis, Massachusetts Institute of Technology]. Retrieved from <http://hdl.handle.net/1721.1/61189>
- Zeping, W., Donghui, W., Weihua, Z., Okolo, P. N., & Yang, F. (2017). Solid-rocket-motor performance-matching design framework. *Journal of Spacecraft and Rockets*, 54(3), 698-707.



© 2026 by the authors. This article is an open access article distributed under the terms and conditions of the Creative Commons Attribution (CC BY-NC-SA) license (<https://creativecommons.org/licenses/by-nc-sa/4.0/>)